

Formation and Reactivity of Some Heterobinuclear Rhodium/Platinum Complexes with 2-(Diphenylphosphino)pyridine as a Bridging Ligand

James P. Farr, Marilyn M. Olmstead, Fred E. Wood, and Alan L. Balch*

Contribution from the Department of Chemistry, University of California, Davis California 95616. Received April 14, 1982

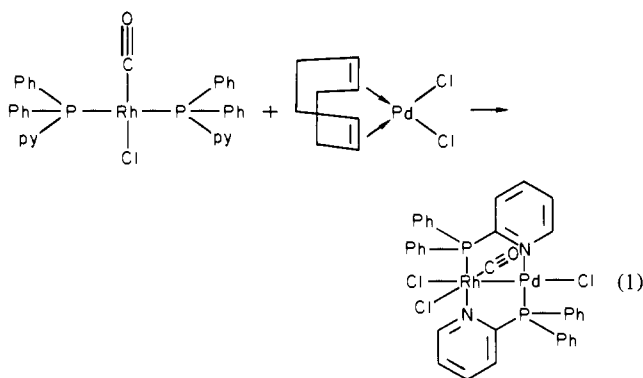
Abstract: Addition of $\text{Rh}_2(\mu\text{-Cl})_2(\text{CO})_4$ to *cis*- $\text{Pt}(\text{Ph}_2\text{Ppy})_2\text{Cl}_2$ forms $[\text{Pt}(\text{Ph}_2\text{Ppy})_2\text{Cl}][\text{Rh}(\text{CO})_2\text{Cl}_2]$, which on heating is converted into $\text{RhPt}(\text{Ph}_2\text{Ppy})_2(\text{CO})\text{Cl}_3$. Treatment of $\text{RhPt}(\text{Ph}_2\text{Ppy})_2(\text{CO})\text{Cl}_3$ with chlorine yields $\text{RhPt}(\text{Ph}_2\text{Ppy})_2(\text{CO})\text{Cl}_5$. Spectroscopic data indicate that the oxidative addition involves only the platinum site and that the rest of the binuclear complex remains intact. Similar preparations of $\text{RhPt}(\text{Ph}_2\text{Ppy})_2(\text{CO})\text{Br}_3$ and $\text{RhPt}(\text{Ph}_2\text{Ppy})_2(\text{CO})\text{I}_3$ are reported. The new compounds have been characterized by infrared and ^{31}P NMR spectroscopy. The ^{195}Pt NMR spectra of $\text{RhPt}(\text{Ph}_2\text{Ppy})_2(\text{CO})\text{X}_3$ are reported: $^1J(\text{Rh}, \text{Pt})$ is 130 Hz for $\text{X} = \text{Cl}$. The structure of $[\text{Pt}(\text{Ph}_2\text{Ppy})_2\text{Cl}][\text{Rh}(\text{CO})_2\text{Cl}_2] \cdot 0.5\text{CH}_2\text{Cl}_2$ has been determined by X-ray crystallography. The compound crystallizes in the space group $P2_12_12_1$ (No. 19) with four cation/anion pairs in the unit cell of dimensions $a = 10.112$ (2), $b = 15.923$ (3), and $c = 24.988$ (5) Å. Full-matrix least-squares refinement yielded $R = 0.053$. The cation contains one monodentate and one chelating Ph_2Ppy ligand.

Binuclear transition-metal complexes and their reaction chemistry have consumed considerable interest in recent times.¹ To a large extent most of the binuclear complexes currently available are symmetric species involving two like metals with identical coordination environments. We have recently been interested in designing complexes in which two different metal centers are present.^{2,3} Such molecules offer attractive potential for catalysis and organometallic-based synthetic chemistry by allowing the two individual metal centers to perform separate, unique functions.

Phosphine ligands, particularly bis(diphenylphosphino)methane (dpm) have proven to be versatile bridging ligands for connecting two metal ions.⁴⁻¹³ While they are capable of bonding relatively firmly to the metal atoms involved, they allow for flexibility in the metal-metal separation and in the coordination geometry about the two metal atoms. In most cases, however, symmetrical complexes result; and so far as we are aware, heterobinuclear complexes have not been made with symmetrical diphosphines.¹⁴

By incorporating a second, different metal-binding site into a phosphine ligand, it is possible to assemble, in a rational manner and high yield, heterobinuclear complexes. 2-(Diphenylphosphino)pyridine^{2,3,15-17} is a particularly useful ligand in this regard, and other ligands of this type are being developed.^{18,19} One

synthesis of a heterobinuclear complex, which proceeds to give 72% yield of pure, crystalline product, is shown in eq 1.² Here



we describe the synthesis of the platinum analogue of **1** by a different route, characterize an intermediate in its formation, and report on some oxidative-addition reactions of the binuclear compound, that involve only the platinum site. These demonstrate that independent reactivity of two different, but closely bound, metal sites in a binuclear complex is possible.

Experimental Section

Preparation of Compounds. 2-(Diphenylphosphino)pyridine was obtained by the established routes.^{17,20}

cis- $\text{Pt}(\text{Ph}_2\text{Ppy})_2\text{Cl}_2$. This compound has been obtained by modification of a standard route to *cis*- $\text{Pt}(\text{Ph}_3\text{P})_2\text{Cl}_2$.²¹ A solution of 1.0 g (2.4 mmol) of K_2PtCl_4 in 15 mL of water was added to a boiling solution of 1.36 g (5.2 mmol) of 2-(diphenylphosphino)pyridine in 20 mL of ethanol. A white precipitate formed immediately. The mixture was heated under reflux for 2 h, cooled, and passed through a sintered-glass filter. The white solid that collected was washed with water, ethanol, and ethyl ether and vacuum dried; yield, 1.4 g, 72%. Anal. Calcd for $\text{C}_{34}\text{H}_{28}\text{Cl}_2\text{N}_2\text{P}_2\text{Pt}$: C, 51.52; H, 3.56; N, 3.53. Found: C, 51.76; H, 3.51; N, 3.60.

$[\text{Pt}(\text{Ph}_2\text{Ppy})_2\text{Cl}][\text{Rh}(\text{CO})_2\text{Cl}_2]$. A solution of 0.110 g (0.25 mmol) of $\text{Rh}_2(\mu\text{-Cl})_2(\text{CO})_4$ in 10 mL of dichloromethane was added dropwise to a solution of 0.45 g (0.57 mmol) of *cis*- $\text{Pt}(\text{Ph}_2\text{Ppy})_2\text{Cl}_2$ in 40 mL of dichloromethane. Ethyl ether was added dropwise to the solution to precipitate the product as yellow crystals. These were collected by filtration, washed with ethyl ether, and vacuum dried. Purification could be achieved by dissolution in dichloromethane and reprecipitation with ethyl ether, yield 0.52 g (93%). In acetone solution the salt has an electrical conductivity of $118 \text{ ohm}^{-1} \text{ cm}^2 \text{ mol}^{-1}$. Anal. Calcd for $\text{C}_{36}\text{H}_{28}\text{Cl}_3\text{N}_2\text{O}_2\text{P}_2\text{PtRh}$: C, 43.81; H, 2.86; N, 2.84. Found: C, 43.68; H, 2.78; N, 2.84.

(15) Farr, J. P.; Olmstead, M. M.; Hunt, C. H.; Balch, A. L. *Inorg. Chem.* **1981**, *20*, 1182-1187.

(16) Olmstead, M. M.; Maisonnat, A.; Farr, J. P.; Balch, A. L. *Inorg. Chem.* **1982**, *21*, 4060-4065.

(17) Maisonnat, A.; Farr, J. P.; Olmstead, M. M.; Hunt, C. T.; Balch, A. L., submitted for publication.

(18) Schore, N. E. *J. Am. Chem. Soc.* **1979**, *101*, 7410-7412.

(19) Rauchfuss, T. B.; Wilson, S. R.; Wroblewski, D. A. *J. Am. Chem. Soc.* **1981**, *103*, 6769-6770.

(20) Mann, F. G.; Watson, J. J. *Org. Chem.* **1948**, *13*, 502-531.

(21) Baller, J. C., Jr.; Hatanl, H. *Inorg. Chem.* **1965**, *4*, 1618-1620.

RhPt(Ph₂Ppy)₂(CO)Cl₃. A solution containing 0.42 g (0.54 mmol) of *cis*-Pt(Ph₂Ppy)₂Cl₂ and 0.10 g (0.27 mmol) of [Rh(CO)₂(μ-Cl)]₂ in 70 mL of benzene was heated under reflux in a nitrogen atmosphere for 5 h and then cooled to room temperature. The orange precipitate that formed was collected by vacuum filtration, washed with 10 mL of methanol, and recrystallized from dichloromethane and ethyl ether to yield 0.35 g (69%) of the product. The conductivity in acetone was 1 ohm⁻¹ cm² mol⁻¹. Anal. Calcd for C₃₅H₂₈Cl₃N₂P₂PtRh: C, 43.80; H, 2.94; N, 2.92. Found: C, 43.27; H, 2.90; N, 2.84.

RhPt(Ph₂Ppy)₂(CO)Cl₃. A solution containing 0.21 g (0.21 mmol) of RhPt(Ph₂Ppy)₂(CO)Cl₃ in 30 mL of dichloromethane was treated with 10 mL of a dichloromethane solution that had been previously saturated with chlorine. The solution turned a deeper red as the chlorine solution was added. The mixture was then evaporated to dryness under vacuum. The orange solid was collected and dried under vacuum; yield 0.22 g, 99%. Anal. Calcd for C₃₅H₂₈Cl₃N₂OP₂PtRh: C, 40.82; H, 2.74; N, 2.72. Found: C, 40.53; H, 2.75; N, 2.82.

Pt(Ph₂Ppy)₂Br₂. A solution of 0.5 g of potassium bromide in 200 mL of 95% ethanol was added to a solution of 0.5 g of Pt(Ph₂Ppy)₂Cl₂ in 200 mL of hot 95% ethanol. The resulting mixture was stirred for 4 h. The solution was filtered and its volume reduced under vacuum on a rotary evaporator until a pale orange solid began to form. Water (10 mL) was added to the mixture, and the product, which precipitated, was collected by filtration, washed with hot water, hot ethanol, and ether, and vacuum dried; yield 90%. Anal. Calcd for C₃₄H₂₈Br₂N₂P₂Pt: C, 46.33; H, 3.20; N, 3.18. Found: C, 45.51; H, 3.16; N, 3.00.

RhPt(Ph₂Ppy)₂(CO)Br₃. This compound was prepared from Pt-(Ph₂Ppy)₂Br₂ and Rh₂(μ-Br)₂(CO)₄ by the route described for RhPt-(Rh₂Ppy)₂(CO)Cl₃. The crude product was contaminated with some Rh₂(Ph₂Ppy)₂(μ-CO)Br₂, which was removed by chromatography on silica gel with chloroform as the eluant. The Rh₂(Ph₂Ppy)₂(μ-CO)Br₂ eluted first, followed by RhPt(Ph₂Ppy)₂(CO)Br₃, which was removed from the column by elution with dichloromethane. Anal. Calcd for C₃₅H₂₈Br₃N₂OP₂PtRh: C, 38.09; H, 2.58; N, 2.56. Found: C, 37.70; H, 2.66; N, 2.55.

Physical Measurements. Infrared spectra were recorded on a Perkin-Elmer 180 infrared spectrometer. Electrical conductivities were determined by use of an Industrial Instruments conductivity bridge with 10⁻³ M acetone solution. ¹H, ³¹P{¹H}, and ¹⁹⁵Pt{¹H} NMR spectra were recorded on a Nicolet NT 200 Fourier transform spectrometer at 200, 81, and 43 MHz, respectively. An external 85% phosphoric acid reference was used for ³¹P NMR spectra and the high-frequency positive convention, recommended by IUPAC, has been used for reporting chemical shifts. For ¹⁹⁵Pt NMR spectra, the reference was external aqueous H₂PtCl₆.

X-ray Data Collection. Yellow-orange needles of [Pt(Ph₂Ppy)₂Cl]-[Rh(CO)₂Cl₂]-0.5CH₂Cl₂ were formed by diffusion of diethyl ether into a dichloromethane solution of the compound. A needle of dimensions 0.50 × 0.10 × 0.11 mm was selected for data collection and mounted on the goniometer head for a Syntex P2₁ diffractometer with the needle axis parallel to the ϕ axis. The temperature of the crystal was maintained at 140 K by using a modified LT-1 low-temperature apparatus. Using a combination of rotation and axial photographs and an automatic indexing routine, we assigned the lattice as orthorhombic *P*. Quick scans of the space group determining reflections showed the conditions $h00, h = 2n; 0k0, k = 2n; 00l, l = 2n$. The space group was therefore *P*₂₁₂₁ (No. 19). A typical reflection had a width at half-height on an ω scan of 0.31°. Accurate cell dimensions were obtained from a least-squares fit of 12 reflections with 26° < 2 θ < 42°. Crystal data and a summary of the data collection procedure are given in Table I. The usual corrections for Lorentz and polarization effects were applied to the intensity data. Reduction to *F*_o and $\sigma(F_o)$ were as previously described.²²

Solution and Refinement of the Structure. The positions of the platinum and rhodium atoms were determined from a Patterson map.²³ The remaining atoms were located on successive Fourier maps. Initial full-matrix least-squares refinement converged at *R* = 0.074 for 47 isotropic atoms and 2583 reflections having $F_o^2 > 3\sigma(F_o)$. During this initial refinement, only the real part of the correlation for anomalous dispersion was included for Pt, Rh, Cl, and P atoms. A test was made for the handedness of the crystal by using the program ABSCON. A total of 355 reflections were determined to be enantiomer sensitive, with $\Delta F_{B_j}/\sigma^2(F_o) > 9.0$. Agreement factors for the initial positions (*R* = 0.074) and for their inverse (*R*_M = 0.157) clearly indicated the original choice to be

Table I. Crystal Data and Data Collection Summary for [Pt(pyPPh₂)₂Cl][Rh(CO)₂Cl₂]-0.5CH₂Cl₂

formula weight	1029.38
space group	<i>P</i> ₂ ₁ ₂ ₁ (No. 19)
cell dims, 140 K	
<i>a</i> , Å	10.112 (2)
<i>b</i> , Å	15.923 (3)
<i>c</i> , Å	24.988 (5)
<i>V</i> , Å ³	4023 (1)
<i>Z</i>	4
density, g cm ⁻³	1.70 (calcd) (140 K) 1.78 (exptl) (298 K)
cryst dims, mm	0.11 × 0.10 × 0.50 mm
radiation	Mo K α (λ = 0.71069 Å)
μ , cm ⁻¹	44.3
absorption correction factors	2.09–2.24
2 θ max, deg	45
scan type	ω
scan range, deg	1.3
bkgd counting, deg offset	stationary, 1
unique data measd	2984
unique data used ($F_o^2 > 3\sigma(F_o^2)$)	2583
final no. least-squares parameters	247
<i>R</i>	0.053

correct. Refinement of the structure proceeded with the imaginary part of the correction for anomalous dispersion included. A difference map computed at this stage revealed a molecule of dichloromethane at less than full occupancy. Anisotropic thermal parameters were assigned to Pt, Rh, Cl, P, and O atoms, and the dichloromethane was included at 0.5 occupancy. Refinement of these atoms converged at 0.065. An absorption correction²⁴ was applied to the data, resulting in *R* of 0.064. Final refinement included hydrogen atoms at calculated positions by using a riding model in which the C–H vector is fixed at 0.96 Å and the *U* value for a hydrogen atom is tied to 1.2 times the *U* value for the carbon atom to which it is bonded. Additionally, the site-occupation factor of the dichloromethane molecule of crystallization was allowed to refine as a variable with the *U* values for these atoms fixed at 0.05 Å². With the thermal parameter constrained in this manner, the computed occupancy was 41%. The final *R* value of 0.053 was computed from 247 least-squares parameters, 112 hydrogen atom parameters, and 2583 reflections, yielding a goodness-of-fit of 1.58 and an average shift/esd of 0.017. The weighting scheme employed was $w = 1/\sigma^2(F_o) + 0.001F_o^2$; *R*_w = 0.056. Aside from a few spurious peaks close to Pt and Rh, a final difference map was featureless.

The possibility for misidentification of the nitrogen atom (N(2)) of the uncoordinated pyridyl group was treated as follows. In the early cycles of refinement the nitrogen atom was distinguished from a carbon atom by its unusually small thermal parameter. After the final cycle of refinement, it was again assigned a carbon atom form factor. Additional refinement to convergence led to a thermal parameter for N(2) as a carbon atom of *U* = 0.0033 Å², whereas all other ortho carbon atoms of this ligand had *U*'s ranging from 0.0235 to 0.0395 Å². This leads to the conclusion that the pyridine nitrogen has been correctly located. Positional parameters for all non-hydrogen atoms are given in Table II. Selected bond distances and angles are given in Tables III and IV. Tables of thermal parameters, hydrogen atom positions, *F*_o, and *F*_c are available as supplementary material.

Results

Synthesis and Spectroscopic Characterization of [Pt-(Ph₂Ppy)₂Cl][Rh(CO)₂Cl₂]. Our initial attempts to obtain the heterobinuclear complex RhPt(Ph₂Ppy)₂(CO)Cl₃ involved an analogous route² to that used for the synthesis of the palladium counterpart. However the reaction between (1,5-COD)PtCl₂ and *trans*-Rh(Ph₂Ppy)₂(CO)Cl produced Rh₂(Ph₂Ppy)₂(μ-CO)Cl₂¹⁵ and *cis*-Pt(Ph₂Ppy)₂Cl₂ instead of the desired product. We then reversed the order in which we bound these metals to Ph₂Ppy. To do this, we made a Pt(II) complex of Ph₂Ppy.

cis-Pt(Ph₂Ppy)₂Cl₂ has been obtained from the reaction of Ph₂Ppy with either PtCl₄²⁻ or (1,5-COD)PtCl₂. Spectroscopic properties, including the value of *J*(Pt, P),²⁵ the similarity of ³¹P NMR parameters to those of *cis*-Pt(Ph₃P)₂Cl₂, and the observation

(22) Balch, A. L.; Benner, L. S.; Olmstead, M. M. *Inorg. Chem.* **1979**, *18*, 2996–3003.

(23) Computer programs used were local versions of Patterson, Fourier, ABSCON, NFMLS (noncentrosymmetric full-matrix least squares), and the SHELXTL, July 1981, program library. Computers were CDC 7600 and Data General Eclipse.

(24) The method obtains an empirical absorption tensor from an expression relating *F*_o and *F*_c: Hope, H.; Moezli, B., unpublished results.

(25) Pregosin, P. S.; Kunz, R. H. ³¹P and ¹³C NMR of Transition Metal Phosphine Complexes"; Springer Verlag: New York, 1979.

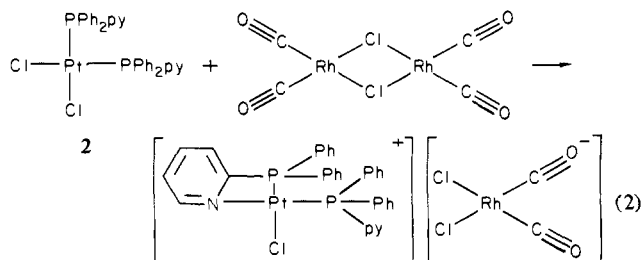
Table II. Atom Coordinates ($\times 10^4$) and Temperature Factors ($\text{\AA}^2 \times 10^3$) for $[\text{Pt}(\text{Ph}_2\text{Ppy})_2\text{Cl}][\text{Rh}(\text{CO})_2\text{Cl}_2] \cdot 0.5\text{CH}_2\text{Cl}_2$

atom	x	y	z	U
Pt	953.2 (8)	613.6 (5)	1878.3 (3)	14.8 (2) ^a
Rh	1016 (2)	590 (1)	-154.5 (6)	24.0 (5) ^a
Cl(1)	-1303 (5)	599 (5)	-232 (2)	36 (2) ^a
Cl(2)	1212 (6)	1754 (4)	-722 (2)	31 (2) ^a
Cl(3)	-1224 (5)	121 (3)	1923 (3)	24 (2) ^a
Cl(4)	5927 (23)	6994 (13)	812 (8)	70
Cl(5)	3329 (22)	7239 (14)	517 (9)	70
P(1)	2835 (6)	1272 (4)	1689 (2)	17 (2) ^a
P(2)	1563 (6)	-159 (4)	2581 (2)	18 (2) ^a
O(1)	3924 (16)	631 (12)	-148 (7)	44 (6) ^a
O(2)	857 (25)	-884 (17)	585 (8)	86 (10) ^a
C(1)	2782 (21)	620 (15)	-135 (8)	20 (5)
C(2)	858 (27)	-334 (15)	300 (10)	32 (6)
C(3)	1822 (21)	1849 (14)	1199 (8)	20 (5)
C(4)	-463 (22)	1738 (14)	965 (8)	21 (5)
C(5)	-257 (26)	2354 (16)	617 (10)	32 (6)
C(6)	966 (26)	2806 (15)	557 (9)	29 (6)
C(7)	2020 (26)	2517 (15)	844 (10)	33 (6)
C(8)	3351 (21)	2103 (13)	2145 (8)	13 (5)
C(9)	2345 (25)	2446 (15)	2441 (9)	31 (6)
C(10)	2583 (26)	3052 (15)	2826 (9)	31 (6)
C(11)	3895 (25)	3319 (15)	2894 (9)	29 (6)
C(12)	4984 (25)	2957 (15)	2621 (9)	30 (6)
C(13)	4659 (27)	2279 (18)	2235 (11)	40 (7)
C(14)	4153 (21)	806 (12)	1288 (7)	15 (5)
C(15)	5138 (21)	1257 (15)	1054 (8)	22 (5)
C(16)	6129 (22)	902 (12)	734 (8)	18 (5)
C(17)	6070 (31)	-12 (18)	698 (11)	52 (8)
C(18)	5070 (19)	-426 (13)	906 (8)	15 (5)
C(19)	4087 (24)	-90 (13)	1206 (8)	23 (5)
C(20)	659 (24)	74 (15)	3187 (10)	33 (6)
C(21)	-490 (23)	-410 (15)	3305 (9)	27 (6)
C(22)	-1194 (27)	-239 (16)	3770 (10)	39 (7)
C(23)	-759 (23)	430 (14)	4077 (9)	30 (6)
C(24)	265 (29)	949 (19)	3974 (11)	49 (8)
C(25)	999 (25)	771 (14)	3501 (9)	32 (6)
C(26)	3314 (2)	-10 (14)	2791 (8)	17 (5)
C(27)	5358 (23)	351 (14)	2490 (9)	26 (6)
C(28)	5928 (29)	75 (16)	2951 (9)	38 (6)
C(29)	5166 (25)	-256 (16)	3360 (10)	33 (6)
C(30)	3796 (25)	-286 (15)	3260 (10)	33 (6)
C(31)	1439 (21)	-1269 (13)	2461 (8)	18 (5)
C(32)	1690 (22)	-1873 (15)	2863 (9)	23 (6)
C(33)	1684 (26)	-2715 (18)	2765 (11)	40 (7)
C(34)	1467 (22)	-3013 (16)	2254 (9)	29 (6)
C(35)	1216 (21)	-2375 (13)	1820 (9)	22 (5)
C(36)	1260 (24)	-1494 (16)	1948 (27)	38 (6)
C(37)	4285 (70)	6674 (45)	948 (27)	50
N(1)	636 (16)	1447 (10)	1254 (6)	10 (4)
N(2)	4080 (18)	308 (10)	2402 (6)	18 (4)

^a Equivalent isotropic defined as one-third of the trace of the orthogonalized U_{ij} tensor.

of two terminal Pt-Cl stretching vibrations in the infrared indicate that the compound exists as the cis isomer. The relevant data are shown in Table V. The bromo analogue, $\text{Pt}(\text{Ph}_2\text{Ppy})_2\text{Br}_2$, has been obtained from $\text{Pt}(\text{Ph}_2\text{Ppy})_2\text{Cl}_2$ by metathesis with sodium bromide.

The reaction of *cis*- $\text{Pt}(\text{Ph}_2\text{Ppy})_2\text{Cl}_2$ with $\text{Rh}_2(\mu\text{-Cl})_2(\text{CO})_4$ (eq 2) in dichloromethane solution occurs rapidly and produces a nearly quantitative yield of the salt, $[\text{Pt}(\text{Ph}_2\text{Ppy})_2\text{Cl}][\text{Rh}(\text{CO})_2\text{Cl}_2]$ (2). In acetone solution it has a conductivity appropriate for a

Table III. Bond Lengths (\AA) in $[\text{Pt}(\text{Ph}_2\text{Ppy})_2\text{Cl}][\text{Rh}(\text{CO})_2\text{Cl}_2]$

Pt-Cl(3)	2.340 (5)	Pt-P(1)	2.223 (6)
Pt-P(2)	2.232 (6)	Pt-N(1)	2.07 (2)
Rh-Cl(1)	2.353 (5)	Rh-Cl(2)	2.342 (6)
Rh-C(1)	1.79 (2)	Rh-C(2)	1.86 (2)
Cl(4)-C(37)	1.73 (7)	Cl(5)-C(37)	1.62 (7)
P(1)-C(3)	1.84 (2)	P(1)-C(8)	1.82 (2)
P(1)-C(14)	1.82 (2)	P(2)-C(20)	1.80 (2)
P(2)-C(26)	1.86 (2)	P(2)-C(31)	1.80 (2)
O(1)-C(1)	1.15 (3)	O(2)-C(2)	1.13 (3)
C(3)-C(7)	1.40 (3)	C(3)-N(1)	1.37 (3)
C(4)-C(5)	1.32 (3)	C(4)-N(1)	1.40 (3)
C(5)-C(6)	1.43 (4)	C(6)-C(7)	1.36 (3)
C(8)-C(9)	1.37 (3)	C(8)-C(13)	1.37 (3)
C(9)-C(10)	1.38 (3)	C(10)-C(11)	1.40 (4)
C(11)-C(12)	1.42 (3)	C(12)-C(13)	1.48 (4)
C(14)-C(15)	1.36 (3)	C(14)-C(19)	1.44 (3)
C(15)-C(16)	1.40 (3)	C(16)-C(17)	1.46 (3)
C(17)-C(18)	1.31 (4)	C(18)-C(19)	1.35 (3)
C(20)-C(21)	1.42 (3)	C(20)-C(25)	1.40 (3)
C(21)-C(22)	1.39 (3)	C(22)-C(23)	1.38 (3)
C(23)-C(24)	1.35 (4)	C(24)-C(25)	1.40 (4)
C(26)-C(30)	1.34 (3)	C(26)-N(2)	1.34 (3)
C(27)-C(28)	1.36 (3)	C(27)-N(2)	1.31 (3)
C(28)-C(29)	1.38 (4)	C(29)-C(30)	1.40 (4)
C(31)-C(32)	1.41 (3)	C(31)-C(36)	1.40 (3)
C(32)-C(33)	1.36 (4)	C(33)-C(34)	1.38 (4)
C(34)-C(35)	1.50 (3)	C(35)-C(36)	1.43 (3)

Table IV. Bond Angles (deg) in $[\text{Pt}(\text{Ph}_2\text{Ppy})_2\text{Cl}][\text{Rh}(\text{CO})_2\text{Cl}_2]$

Cl(3)-Pt-P(1)	166.8 (2)	Cl(3)-Pt-P(2)	92.2 (2)
P(1)-Pt-P(2)	101.0 (2)	Cl(3)-Pt-N(1)	96.0 (5)
P(1)-Pt-N(1)	70.8 (5)	P(2)-Pt-N(1)	171.1 (5)
Cl(1)-Rh-Cl(2)	91.7 (2)	Cl(1)-Rh-C(1)	176.3 (7)
Cl(2)-Rh-C(1)	84.9 (7)	Cl(1)-Rh-C(2)	88.2 (9)
Cl(2)-Rh-C(2)	179.8 (8)	C(1)-Rh-C(2)	95.2 (11)
Pt-P(1)-C(3)	84.3 (7)	Pt-P(1)-C(8)	117.0 (7)
C(3)-P(1)-C(8)	102.3 (10)	Pt-P(1)-C(14)	123.4 (7)
C(3)-P(1)-C(14)	104.1 (9)	C(8)-P(1)-C(14)	115.4 (10)
Pt-P(2)-C(20)	114.0 (8)	Pt-P(2)-C(26)	114.5 (7)
C(20)-P(2)-C(26)	102.7 (10)	Pt-P(2)-C(31)	113.0 (7)
C(20)-P(2)-C(31)	107.8 (11)	C(26)-P(2)-C(31)	103.8 (10)
Rh-C(1)-O(1)	176.8 (18)	Rh-C(2)-O(2)	174.9 (26)
P(1)-C(3)-C(7)	136.1 (18)	P(1)-C(3)-N(1)	100.8 (14)
C(7)-C(3)-N(1)	123.1 (2)	C(5)-C(4)-N(1)	117.2 (20)
C(4)-C(5)-C(6)	125.0 (23)	C(5)-C(6)-C(7)	116.7 (21)
C(3)-C(7)-C(6)	118.4 (23)	P(1)-C(8)-C(9)	114.4 (16)
P(1)-C(8)-C(13)	121.8 (17)	C(9)-C(8)-C(13)	123.1 (21)
C(8)-C(9)-C(10)	121.6 (23)	C(9)-C(10)-C(11)	117.4 (22)
C(10)-C(11)-C(12)	123.5 (22)	C(11)-C(12)-C(13)	115.9 (22)
C(8)-C(13)-C(12)	117.9 (23)	P(1)-C(14)-C(15)	123.8 (16)
P(1)-C(14)-C(19)	116.5 (15)	C(15)-C(14)-C(19)	119.6 (19)
C(14)-C(15)-C(16)	123.7 (21)	C(15)-C(16)-C(17)	114.2 (21)
C(16)-C(17)-C(18)	120.5 (25)	C(17)-C(18)-C(19)	125.7 (22)
C(14)-C(19)-C(18)	115.9 (20)	P(2)-C(20)-C(21)	118.3 (18)
P(2)-C(20)-C(25)	120.5 (18)	C(21)-C(20)-C(25)	120.9 (22)
C(20)-C(21)-C(22)	119.9 (22)	C(21)-C(22)-C(23)	116.8 (23)
C(22)-C(23)-C(24)	127.5 (24)	C(23)-C(24)-C(25)	115.9 (25)
C(20)-C(25)-C(24)	119.6 (23)	P(2)-C(26)-C(30)	123.2 (17)
P(2)-C(26)-N(2)	113.2 (15)	C(30)-C(26)-N(2)	123.1 (20)
C(28)-C(27)-N(2)	122.8 (22)	C(27)-C(28)-Cl(29)	120.8 (26)
C(28)-C(29)-C(30)	115.4 (23)	C(26)-C(30)-C(29)	120.0 (22)
P(2)-Cl(31)-C(32)	122.5 (16)	P(2)-Cl(31)-C(36)	114.9 (17)
C(32)-C(31)-C(36)	122.0 (21)	C(31)-C(32)-C(33)	122.7 (22)
C(32)-C(33)-C(34)	120.4 (24)	C(33)-C(34)-C(35)	117.4 (22)
C(34)-C(35)-C(36)	121.8 (21)	C(31)-C(36)-C(35)	115.5 (22)
Cl(4)-C(37)-Cl(5)	110.4 (41)	Pt-N(1)-C(3)	103.9 (12)
Pt-N(1)-C(4)	136.2 (13)	C(3)-N(1)-C(4)	119.1 (17)
C(26)-N(2)-C(27)	117.8 (18)		

1:1 electrolyte.²⁶ The infrared spectrum is consistent with the presence of $\text{Rh}(\text{CO})_2\text{Cl}_2^-$, which is a well-known and quite stable anion. In $[\text{Ph}_4\text{As}][\text{Rh}(\text{CO})_2\text{Cl}_2]$, the anion displays very strong carbonyl stretching vibrations at 2060 and 1975 cm^{-1} ,²⁷ while in

(26) Geary, W. J. *Coord. Chem. Rev.* 1971, 7, 81-122.

(27) Vallarino, L. M. *Inorg. Chem.* 1965, 4, 161-165.

Table V. Spectroscopic Properties of 2-(Diphenylphosphino)pyridine Complexes

compound	$^{31}\text{P}\{^1\text{H}\}$ NMR spectra ^a						infrared spectra, ^a cm^{-1}	
	δ		J , Hz					
	Pt-P	Rh-P	$^1J_{\text{Rh-P}}$	$^2J_{\text{Rh-P}}$	$^1J_{\text{Pt-P}}$	$^2J_{\text{Pt-P}}$		$^3J_{\text{P-P}}$
<i>cis</i> -Pt(Ph ₂ Ppy) ₂ Cl ₂	11.62				3675.6			312, 283, $\nu(\text{Pt-Cl})^b$
Pt(Ph ₃ P) ₂ Cl ₂	14.92				3673			
Pt(Ph ₂ Ppy) ₂ Br ₂	10.86 (br)				3618			
[Pt(Ph ₂ Ppy) ₂ Cl] ⁺	15.24				3704			2068, 1989, $\nu(\text{C}\equiv\text{O})$
[Rh(CO) ₂ Cl ₂]	-50.3				3339			
RhPt(Ph ₂ Ppy) ₂ (CO)Cl ₃	1.04	24.6	114	2.9	4035	~133	14.0	2055, $\nu(\text{C}\equiv\text{O})$
RhPd(Ph ₂ Ppy) ₂ (CO)Cl ₃	16.1	21.9	113	2.3			17.4	2052, $\nu(\text{C}\equiv\text{O})$
RhPt(Ph ₂ Ppy) ₂ (CO)Cl ₂	-17.9	27.9	110		2793.3	63.0	19.7	2082, $\nu(\text{C}\equiv\text{O})$
RhPt(Ph ₂ Ppy) ₂ (CO)Br ₃	0.13	24.0	110		3950		15	2060, $\nu(\text{C}\equiv\text{O})$
RhPt(Ph ₂ Ppy) ₂ (CO)Br ₂	-20.7	27.6	112		2776	368	15	3077, $\nu(\text{C}\equiv\text{O})$

^a In dichloromethane solutions unless otherwise noted. ^b In Nujol mull.

[Pt(Ph₂Ppy)₂Cl][Rh(CO)₂Cl₂], corresponding features occur at 2068 and 1989 cm^{-1} . The ^{31}P NMR spectrum of the cation consists of two resonances, each with two satellites due to ^{195}Pt (spin = $1/2$, 33.4% natural abundance). The magnitude of each $^1J(\text{Pt-P})$ is consistent with the presence of Pt(II).¹³ The lack of detectable P-P coupling in the cation suggests that the two phosphorus ligands are *cis*. When inequivalent *trans* phosphine ligands are present, the P-P coupling constant is expected to be about 300 Hz, whereas *cis* P-P coupling constants can be vanishingly small.²⁵ Of the two ^{31}P NMR resonances, the one at -50.3 ppm is most likely the one due to the chelating phosphine. In an analogous chelated complex Ru(Ph₂Ppy)(CO)₂Cl₂, a shift of the ^{31}P NMR resonance to low frequency relative to the free ligand (-3.36 ppm) was noted.¹⁶ The magnitude of the coordination shift in Pt(Ph₂Ppy)₂Cl⁺ is much larger than in Ru(Ph₂Ppy)(CO)₂Cl₂, but shifts to low frequency are uncommon. Generally, coordination of a phosphine ligand produces a shift of the ^{31}P resonance to high frequency. Similar shifts of ^{31}P resonances to low frequency are seen in *ortho*-metalated triphenylphosphine complexes that contain strained four-membered rings.

Crystal Structure of [(Ph₂Ppy)₂PtCl][Rh(CO)₂Cl₂·0.5CH₂Cl₂]. The salt crystallized with one cation, one anion, and one-half of a dichloromethane molecule in the asymmetric unit. There is no crystallographic symmetry imposed on either the cation or the anion. Final atomic coordinates are listed in Table II. Selected interatomic distances and angles are given in Tables III and IV.

The anion, which is well-known, is planar. The structural parameters agree with those obtained in previous structure determinations on different salts containing this ion.²⁸⁻³¹

A drawing of the cation with the numbering scheme is shown in Figure 1. Figure 2 shows a stereoscopic drawing of the cation. The coordination about the platinum is planar. One of the phosphine ligands is chelating through its nitrogen and phosphorus atoms while the other functions as a monodentate, P-bound ligand. The two phosphorus atoms are *cis* to one another. A terminal chloride completes the coordination sphere. The metal-ligand distances all appear normal. The two different Pt-P bonds have the same lengths. The Pt-P and Pt-Cl distances are comparable to those in *cis*-(Me₃P)₂PtCl₂.³²

Because of the presence of the four-membered chelate ring, the angles at platinum between *cis* ligands deviate from the ideal value of 90°. The major deviation comes from P(1)-Pt-N(1), which is only 70.6°. As a result of this compression, the two adjacent angles have opened up so that N(1)-Pt-Cl(3) is 96.4° and P-

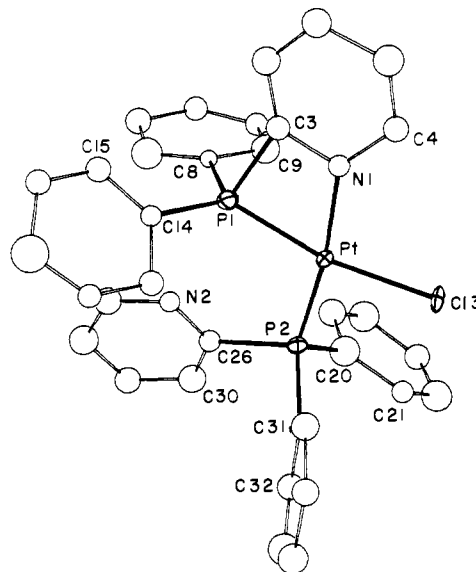


Figure 1. Drawing of [Pt(Ph₂Ppy)₂Cl]⁺ showing the numbering system.

(1)-Pt-P(2) is 101.0°. On the other hand, the angle between the two *cis* monodentate ligands (that is, P(2)-Pt-Cl(3)) is 91.9°, nearly the ideal value.

Within the chelate ring there is also significant angular compression. This may be seen in the lower part of Figure 3, where a cross section of the plane of this ring is shown. Both the C(3)-N(1)-Pt and N(1)-C(3)-P(1) angles (104.0° and 101.7°, respectively) are reduced from the ideal value of 120°, and the C(3)-P(1)-Pt angle of 84° is reduced below the expected value of 109.5°. The angular compression seen in this ring is very similar to that found in the chelate ring of (Ph₂Ppy)Ru(CO)₂Cl₂.¹⁶ A comparison of the two chelate rings is made in Figure 3. We have noted previously that these angular compressions are similar to those found in *ortho*-metalated triphenylphosphine complexes.¹⁶

The cation/anion interactions in the crystalline salt have been analyzed to see what clues the solid-state structure might give about how the binuclear, metal-metal bonded complex RhPt-(Ph₂Ppy)₂(CO)Cl₃ is formed from these ions. Two features of the structure have commanded our attention. First, the distances between N(2), the uncoordinated nitrogen atom, and neighboring rhodium atoms were examined. The shortest distance is 6.272 Å, well beyond that needed for any significant bonding or incipient bonding to be occurring. In fact, N(2) is much closer (3.45 Å) to the platinum atom within the cation than it is to any rhodium atom. Second, the platinum to rhodium interatomic distances have been examined. The closest of these involves a 5.080-Å separation between the two metal atoms. The next closest approaches of anions to the cations involve Pt...Rh distances of 8.249, 8.946, and 9.017 Å. In comparison, the closest approach to two cations results in a 8.761-Å separation of two platinum atoms. Consequently, we have focused our attention on the unique, closely spaced

(28) Thomas, C. K.; Stanko, J. A. *Inorg. Chem.* **1971**, *10*, 566.

(29) Einstein, F. W. B.; Hampton, C. R. S. M. *Can. J. Chem.* **1971**, *49*, 1901.

(30) Cetinkaya, E.; Johnson, A. W.; Lappert, M. F.; McLaughlin, G. M.; Muir, K. W. *J. Chem. Soc., Dalton Trans.* **1973**, 1236.

(31) For example, the reaction of Rh₂(μ-dpm)₂(CO)₂Cl₂ with Rh₂(μ-Cl)₂(CO)₄ produces [Rh₂(μ-dpm)₂(μ-Cl)(CO)₂]⁺[Rh(CO)₂Cl₂]⁻: Olmstead, M. M.; Lindsay, C. H.; Benner, L. S.; Balch, A. L. *J. Organomet. Chem.* **1979**, *179*, 293-300.

(32) Messmer, G. G.; Amma, E. L.; Ibers, J. A. *Inorg. Chem.* **1967**, *6*, 725-730.

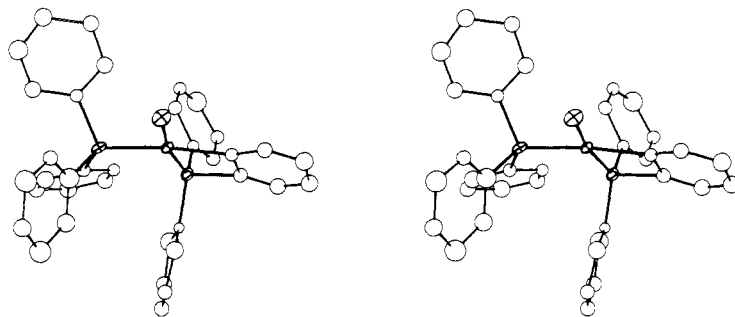


Figure 2. Stereoscopic view of the complex cation $[\text{Pt}(\text{Ph}_2\text{Ppy})_2\text{Cl}]^+$.

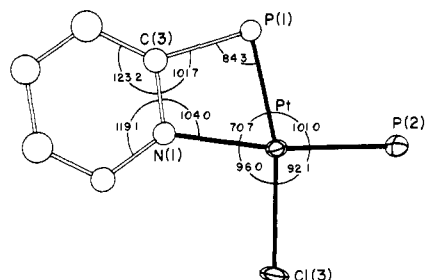
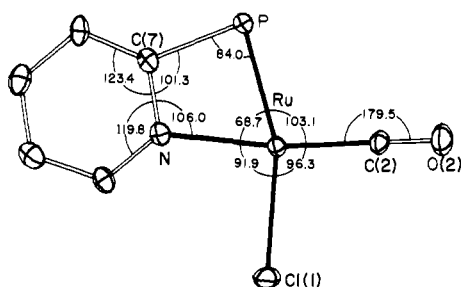


Figure 3. Comparison of the planar chelating ligands in $\text{Ru}(\text{Ph}_2\text{Ppy})(\text{CO})_2\text{Cl}_2$ (top) and $[\text{Pt}(\text{Ph}_2\text{Ppy})_2\text{Cl}]^+$ (bottom).

cation/anion pair. A diagram showing this cation/anion contact is given in Figure 4. In this cation/anion pair, the rhodium atom sits atop the pyridine ring of the chelated 2-(diphenylphosphino)pyridine ligand. The angle between the normals to the planes of the cation and anion is only 13.6° , so these planar ions lie nearly parallel to one another. The rhodium is not centered over the pyridine ring but is closest to C(4) and C(5) of the ring. The distance from the rhodium atom to the ring plane is 3.55 \AA , and the Rh-C distances range from 4.08 to 3.66 \AA . For comparison, the rhodium-phenyl distances in two complexes where an arene is actually coordinated to rhodium are available. In $\{(\text{MeO})_3\text{P}\}_2\text{Rh}(\eta^6\text{-Ph})\text{BPh}_3$, the rhodium atom is centered 1.86 \AA above the plane of the phenyl ring and the Rh-C distances range from 2.30 to 2.41 \AA .³³ In $\text{Rh}_2(\text{Ph}_2\text{PCH}_2\text{CH}_2\text{PPh}_2)_2^{2+}$, again the rhodium atom is centered over a phenyl group and the Rh-C distances range from 2.285 to 2.368 \AA .³⁴ Consequently, it is certain that the arene is not coordinated in the usual sense to the rhodium ion of $\text{Rh}(\text{CO})_2\text{Cl}_2^-$. Note that the geometry of the anion itself does not appear to be significantly altered from that seen in other salts.²⁸⁻³¹ While this exact structure of the cation/anion pair is unlikely to persist in solution, we feel that the plane of the chelating portion of the phosphinopyridine ligand along with coulombic and charge-transfer effects may serve to conduct the rhodium-containing anion toward the platinum atom so that the formation of the binuclear compound is facilitated.

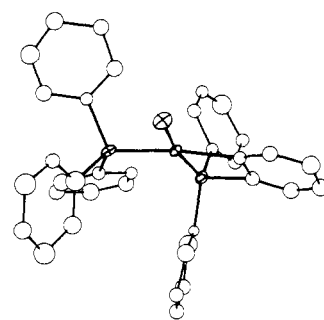
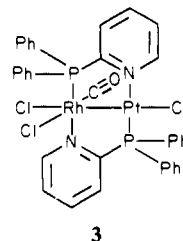


Figure 4. Projection showing the overlap of the planar portions of the cation/anion pair in $[\text{Pt}(\text{Ph}_2\text{Ppy})_2\text{Cl}][\text{Rh}(\text{CO})_2\text{Cl}_2]$.

Preparation of $\text{RhPt}(\text{Ph}_2\text{Ppy})_2(\text{CO})\text{Cl}_3$. Heating $[\text{Pt}(\text{Ph}_2\text{Ppy})_2\text{Cl}][\text{Rh}(\text{CO})_2\text{Cl}_2]$ in benzene converts it into $\text{RhPt}(\text{Ph}_2\text{Ppy})_2(\text{CO})\text{Cl}_3$ (**3**), which has been isolated as orange crystals.



This compound is a nonelectrolyte in acetone solution. The infrared absorption at 2055 cm^{-1} indicates that the single carbonyl group occupies a terminal position.

$\text{RhPt}(\text{Ph}_2\text{Ppy})_2(\text{CO})\text{Br}_3$ has been obtained from the reaction between $\text{Pt}(\text{Ph}_2\text{Ppy})_2\text{Br}_2$ and $\text{Rh}_2(\mu\text{-Br})_2(\text{CO})_4$. Its spectroscopic properties are similar to those of its chloro analogue.

The $^{31}\text{P}\{^1\text{H}\}$ NMR spectrum of $\text{RhPt}(\text{Ph}_2\text{Ppy})_2(\text{CO})\text{Cl}_3$ is shown in Figure 5. The two inequivalent phosphorus resonances centered at 24.6 and 1.04 ppm are apparent. The one at 24.6 is due to the rhodium-bound phosphorus and appears as a set of four equally intense lines due to coupling to ^{103}Rh (spin $1/2$, 100% natural abundance) as well as coupling to the second phosphorus. In addition, weak satellites are seen that come from two-bond coupling of the phosphorus to the platinum. The platinum-bound phosphorus atom shows a quartet centered at 1.04 ppm due to splitting from $^2J(\text{Rh}, \text{P})$ and $^3J(\text{P}, \text{P})$. Satellites due to the splitting from ^{195}Pt are readily visible at low frequency while the other set of satellites at high frequency nearly overlaps with the rhodium-bound phosphorus resonance pattern at 24.6 ppm. The magnitudes of the various coupling constants ($^1J(\text{Rh}-\text{P})$, $^2J(\text{Rh}-\text{P})$, and $^3J(\text{P}, \text{P})$) compare well with those found in $\text{RhPd}(\text{Ph}_2\text{Ppy})_2(\text{CO})\text{Cl}_3$. These are given in Table V for comparison.

The formation of **3** can be viewed in formal terms as an oxidation of rhodium(I) to rhodium(II) and reduction of platinum(II) to platinum(I). The magnitudes of $^2J(\text{Pt}, \text{P})$ and $^2J(\text{Rh}, \text{P})$, when compared to those of corresponding Rh(I) and Pt(II) compounds, are consistent with these changes. The magnitude of one-bond metal-phosphorus coupling constants generally increases as the oxidation state decreases. Correspondingly, $^2J(\text{Pt}-\text{P})$ in **3** is larger

(33) Nolte, M. J.; Gafner, G.; Haines, L. M. *J. Chem. Soc., Chem. Commun.* **1968**, 1406-1407.

(34) Halpern, J.; Riley, D. P.; Chan, A. S. C.; Pluth, J. J. *J. Am. Chem. Soc.* **1977**, *99*, 8055-8057.

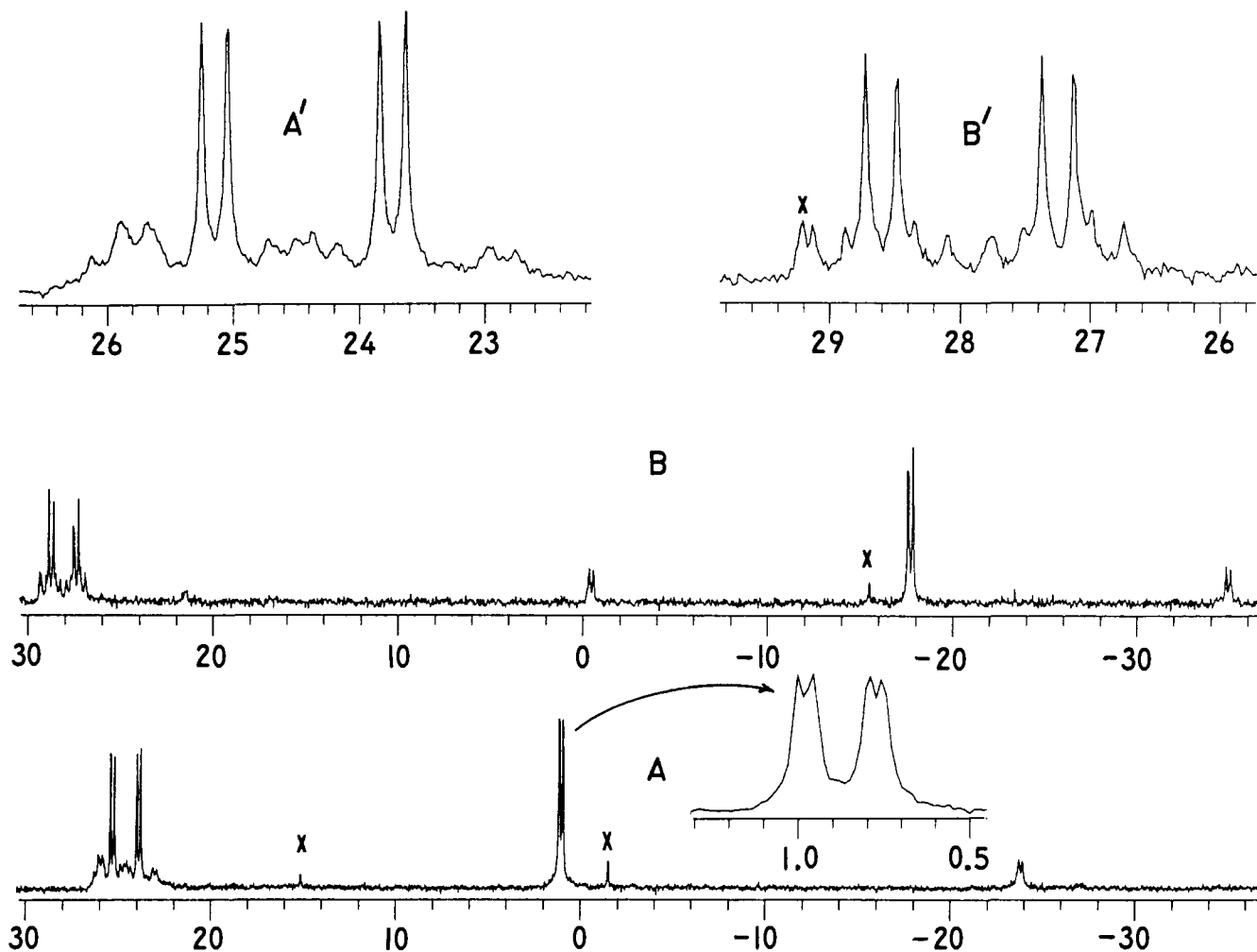


Figure 5. $^{31}\text{P}\{^1\text{H}\}$ NMR spectra of (A) $\text{RhPt}(\text{Ph}_2\text{Ppy})_2(\text{CO})\text{Cl}_3$ and (B) $\text{RhPt}(\text{Ph}_2\text{Ppy})_2(\text{CO})\text{Cl}_5$ in dichloromethane solution at 25 °C. The insets at the top show expansions of the downfield regions where the rhodium resonances are centered. X marks impurities.

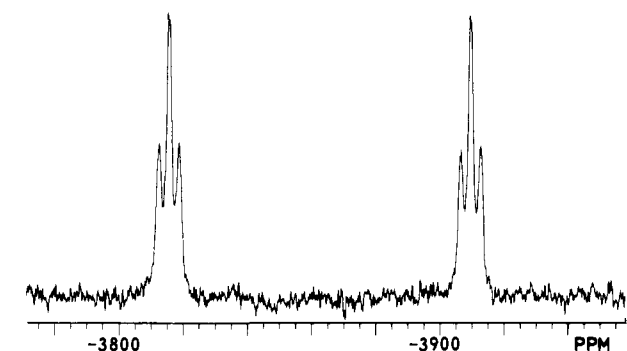


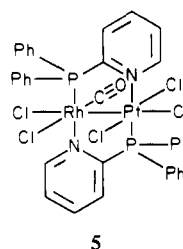
Figure 6. $^{195}\text{Pt}\{^1\text{H}\}$ NMR spectrum of $\text{RhPt}(\text{Ph}_2\text{Ppy})_2(\text{CO})\text{Cl}_3$ in dichloromethane solution at 25 °C.

than it is in any of the Pt(II) compounds in Table V. Likewise, $^2J(\text{Rh}-\text{P})$ in **3** is smaller than $^2J(\text{Rh}-\text{P})$ in $\text{Rh}(\text{Ph}_2\text{Ppy})_2(\text{CO})\text{Cl}$ (127.8 Hz).²

The ^{195}Pt NMR spectrum of $\text{RhPt}(\text{Ph}_2\text{Ppy})_2(\text{CO})\text{Cl}_2$ is shown in Figure 6. The major splitting between the two triplets is due to the $^1J(\text{Pt}, \text{P})$, and the value of 4027 Hz obtained from the ^{195}Pt spectrum agrees with the value of 4035 Hz obtained from the ^{31}P NMR spectrum. The triplets arise due to coupling to both the remote phosphorus and the rhodium. The value of $^2J(\text{Pt}, \text{P})$ is known to be 133 Hz from the ^{31}P NMR spectrum, and the observed splitting in the ^{195}Pt NMR is 130 Hz. Consequently, $^1J(\text{Pt}, \text{Rh})$ must have a similar magnitude to produce the triplet pattern in the ^{195}Pt NMR spectrum. The only other systems whose $^1J(\text{Pt}, \text{Rh})$ has been observed are the cluster compounds $[\text{Rh}_3\text{Pt}(\text{CO})_{15}]^-$, $^1J(\text{Pt}, \text{Rh}) = 24$ Hz, and $[\text{Rh}_2\text{Pt}(\text{CO})_x]^-$, $^1J(\text{Pt}, \text{Rh}) = 55$ Hz.³⁵

These show smaller values for this coupling constant.

Oxidative Additions to $\text{RhPt}(\text{Ph}_2\text{Ppy})_2(\text{CO})\text{X}_3$. Chlorine adds readily to **3** to form $\text{RhPt}(\text{Ph}_2\text{Ppy})_2(\text{CO})\text{Cl}_5$ (**5**), which has been



isolated as orange crystals. The product is a nonelectrolyte in dichloromethane solution. The spectroscopic properties reveal that oxidation has affected only one of the two metal centers. The carbonyl stretching frequency, which is a convenient probe of the electron density at the rhodium center, shows only a slight increase of 27 cm^{-1} upon oxidative addition. For comparison, halogen oxidation of rhodium(I) complexes to rhodium(III) complexes usually results in an increase of about 100 cm^{-1} for the carbonyl stretching frequency, while the oxidation of dimeric rhodium(I) complexes to dimeric rhodium(II) complexes results in an analogous increase of 60 cm^{-1} .³⁶

The $^{31}\text{P}\{^1\text{H}\}$ NMR spectrum of $\text{RhPt}(\text{Ph}_2\text{Ppy})_2(\text{CO})\text{Cl}_5$ also reveals considerable consistency in the parameters affecting the

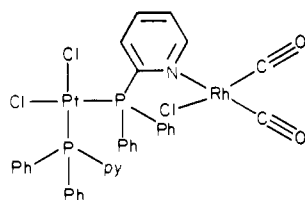
(35) Fumagalli, A.; Martinengo, S.; Chini, P.; Albinati, A.; Bruckner, S.; Heaton, B. T. *J. Am. Chem. Soc., Chem. Commun.* **1978**, 195-196.
(36) Balch, A. L. *J. Am. Chem. Soc.* **1976**, *98*, 8049-8054.

rhodium-bound phosphorus atom. The chemical shift of this resonance has experienced a 3.3 ppm shift to high frequency. The magnitudes of $^1J(\text{Rh}, \text{P})$ and $^2J(\text{P}, \text{P})$ have changed only slightly on oxidation. On the other hand, the parameters concerning the platinum-bound phosphorus atom have changed more markedly. There is a sizable alteration in the chemical shift of that phosphorus, and, more significantly, $^1J(\text{Pt}, \text{P})$ has decreased by more than 1200 Hz. Such a shift is fully consistent with oxidative addition centered at the platinum atom.

Addition of bromine to $\text{RhPt}(\text{Rh}_2\text{Ppy})_2(\text{CO})\text{Br}_3$ produces $\text{RhPt}(\text{Ph}_2\text{Ppy})_2(\text{CO})\text{Br}_5$, which has properties similar to those of the chloro analogue. Comparison of the ^{31}P NMR spectral features in Table V clearly shows the congruence of all of the parameters except for $^2J(\text{Pt}, \text{P})$. This parameter changes in an erratic fashion. On addition of chlorine to $\text{RhPt}(\text{Ph}_2\text{Ppy})_2(\text{CO})\text{Cl}_3$ it decreases, while on addition of bromine to $\text{RhPt}(\text{Ph}_2\text{Ppy})_2(\text{CO})\text{Br}_2$ it increases. Unfortunately, the low solubilities of $\text{RhPt}(\text{Ph}_2\text{Ppy})_2(\text{CO})\text{X}_5$ ($\text{X} = \text{Cl}, \text{Br}$) have precluded the acquisition of their ^{195}Pt NMR spectra.

Discussion

Although many polynuclear metal complexes have been synthesized, relatively little is known about the mechanism of their formation. The present work offers insight into one such process by showing that the salt $[\text{Pt}(\text{Ph}_2\text{Ppy})_2\text{Cl}][\text{Rh}(\text{CO})_2\text{Cl}_2]$ is an intermediate on the path to the formation of $\text{RhPt}(\text{Ph}_2\text{Ppy})_2(\text{CO})\text{Cl}_3$. Initially this is somewhat surprising. We had suspected that a species such as **6** would have been a more likely intermediate



6

for several reasons. Pyridine (py) is known to react with $\text{Rh}_2(\mu\text{-Cl})_2(\text{CO})_4$ to form $\text{Rh}(\text{CO})_2(\text{py})\text{Cl}$.³⁷ An analogous reaction of $\text{Pt}(\text{Ph}_2\text{Ppy})_2\text{Cl}_2$ with $\text{Rh}_2(\mu\text{-Cl})_2(\text{CO})_4$ to form **6** would have disrupted the dinuclear structure of $\text{Rh}_2(\mu\text{-Cl})_2(\text{CO})_4$ and would have attached the two metal atoms to a common ligand. We would expect that such an arrangement would facilitate subsequent metal-metal bond formation. However, the reaction actually takes a different course.

In undergoing reaction 2, several important bond changes are accomplished. Not only is the dimeric structure of $\text{Rh}_2(\mu\text{-Cl})_2(\text{CO})_4$ disrupted but the halide transfer from platinum to rhodium is achieved. The ability of $\text{Rh}_2(\mu\text{-Cl})_2(\text{CO})_4$ to abstract halide ion from metal complexes has been seen before.³¹ In addition to accomplishing the halide transfer, ionization also begins the process of reorientation of the phosphine ligand. In the starting materials the two phosphine ligands are mutually cis and bonded through phosphorus to platinum. Ionization proceeds stereospecifically to give the isomeric cation with the pyridine nitrogen atom trans to the monodentate phosphine ligand. This is their relative orientation in the final product. The cation's geometry implies that the pyridine nitrogen has directly replaced the outgoing chloride. The process leaves an uncoordinated nitrogen atom on the cation, and we suspect that in the further reaction it is this nitrogen that initially binds to the rhodium anion to eventually give the metal-metal bonded product. The association between cation and anion is of course assisted by coulombic factors, and we have observed qualitatively that the reaction to form **3** is faster in benzene than it is in methanol, perhaps because ion pairing in the less polar solvents increases the probability of reaction between the cation and the anion.

Once formed, the rhodium-platinum bond in **3** appears quite robust. Certainly the bridging ligands contribute to this. Although oxidation by halogens frequently results in rupture of metal-metal bonds, this does not appear to occur in the transformation of **3** to **5**. In part, the stability of the metal-metal bonded arrangements in **3** and **5** can be attributed to the coordination saturation at one or both metal centers. We have previously shown that the metal-metal bond in $\text{Rh}_2(\text{dpm})_2(\text{CNR})_4\text{X}_2^{2+}$, a coordinatively saturated species, is stable to excess halogen^{36,38} whereas the metal-metal bond in $\text{Pd}_2(\text{dpm})_2\text{X}_2$, an unsaturated species, is readily broken on reaction with halogens.³⁹

Acknowledgment. We thank the National Science Foundation (CHE 7924575) for support. J.P.F. and F.E.W. were Regents of the University of California Fellows.

Registry No. 2-0.5 CH_2Cl_2 , 84074-37-3; **3**, 84074-38-4; **5**, 84074-39-5; *cis*- $\text{Pt}(\text{Ph}_2\text{Ppy})_2\text{Cl}_2$, 38255-47-9; $\text{Rh}_2(\mu\text{-Cl})_2(\text{CO})_4$, 14523-22-9; $\text{Pt}(\text{Ph}_2\text{Ppy})_2\text{Br}_2$, 84074-40-8; $\text{RhPt}(\text{Ph}_2\text{Ppy})_2(\text{CO})\text{Br}_3$, 84074-41-9.

Supplementary Material Available: Structure factor tables, anisotropic thermal parameters, and atomic coordinates for hydrogen atoms for $[\text{Pt}(\text{Ph}_2\text{Ppy})_2\text{Cl}][\text{Rh}(\text{CO})_2\text{Cl}_2]$ (18 pages). Ordering information is given on any current masthead page.

(38) Balch, A. L.; Labadie, J. W.; Delker, G. *Inorg. Chem.* **1979**, *18*, 1224-1227.

(39) Hunt, C. T.; Balch, A. L. *Inorg. Chem.* **1981**, *20*, 2267-2270.

(37) Lawson, D. N.; Wilkinson, G. *J. Chem. Soc.* **1965**, 1900-1907.